

# MAIN DUMP LINE: BEAM LOSS SIMULATIONS WITH THE TDR PARAMETERS

---

Y. Nosochkov

E. Marin, G. White (SLAC)

LCWS14 Workshop, Belgrade, October 7, 2014

# Dump line and beam parameter options

- Extraction line design with  $L_{\text{ex}}^* = 6.3$  m free space after IP.
- SiD solenoid field with and without anti-DID field and with orbit correction downstream of IP.
- 500 GeV and 1 TeV CM energy.
- 14 mrad crossing angle.
- TDR beam parameter options:
  - 500 GeV nominal,
  - 1 TeV options A1 (low beamstrahlung) and B1b (high beamstrahlung – with ~2 times more energy loss compared to A1),
  - head-on collisions,
  - with vertical offset ( $\pm$ ) between the beams at IP adjusted for maximum disruption.
- Disrupted electron and beamstrahlung photon beam distributions at IP generated using Guinea-Pig.
- Beam power loss in the dump line obtained using DIMAD tracking simulations.

# TDR beam parameters

|  |                         | Center-of-mass energy, $E_{\text{cm}}$ (GeV) |       |       |       |          |           |            | Unit  |
|--|-------------------------|--|-------|-------|-------|----------|-----------|------------|---|
|  |                         | Baseline                                     |       |       |       | Upgrades |           |            |   |
| Parameter                                |                         | 200  | 250   | 350   | 500   | 500      | 1000 (A1) | 1000 (B1b) |   |
| Nominal bunch population                 | $N$                     | 2.0  | 2.0   | 2.0   | 2.0   | 2.0      | 1.74      | 1.74       | $\times 10^{10}$                                |
| Pulse frequency                          | $f_{\text{rep}}$        | 5  | 5     | 5     | 5     | 5        | 4         | 4          | Hz  |
| Bunches per pulse                        | $N_{\text{bunch}}$      | 1312   | 1312  | 1312  | 1312  | 2625     | 2450      | 2450       |   |
| Nominal horizontal beam size at IP       | $\sigma_x^*$            | 904  | 729   | 684   | 474   | 474      | 481       | 335        | nm  |
| Nominal vertical beam size at IP         | $\sigma_y^*$            | 7.8  | 7.7   | 5.9   | 5.9   | 5.9      | 2.8       | 2.7        | nm  |
| Nominal bunch length at IP               | $\sigma_z^*$            | 0.3  | 0.3   | 0.3   | 0.3   | 0.3      | 0.250     | 0.225      | mm  |
| Energy spread at IP, $e^-$               | $\delta E/E$            | 0.206  | 0.190 | 0.158 | 0.124 | 0.124    | 0.083     | 0.085      | %   |
| Energy spread at IP, $e^+$               | $\delta E/E$            | 0.190  | 0.152 | 0.100 | 0.070 | 0.070    | 0.043     | 0.047      | %   |
| Horizontal beam divergence at IP         | $\theta_x^*$            | 57   | 56    | 43    | 43    | 43       | 21        | 30         | $\mu\text{rad}$                                 |
| Vertical beam divergence at IP           | $\theta_y^*$            | 23   | 19    | 17    | 12    | 12       | 11        | 12         | $\mu\text{rad}$                                 |
| Horizontal beta-function at IP           | $\beta_x^*$             | 16   | 13    | 16    | 11    | 11       | 22.6      | 11         | mm  |
| Vertical beta-function at IP             | $\beta_y^*$             | 0.34   | 0.41  | 0.34  | 0.48  | 0.48     | 0.25      | 0.23       | mm  |
| Horizontal disruption parameter          | $D_x$                   | 0.2  | 0.3   | 0.2   | 0.3   | 0.3      | 0.1       | 0.2        |   |
| Vertical disruption parameter            | $D_y$                   | 24.3   | 24.5  | 24.3  | 24.6  | 24.6     | 18.7      | 25.1       |   |
| Energy of single pulse                   | $E_{\text{pulse}}$      | 420  | 526   | 736   | 1051  | 2103     | 3409      | 3409       | kJ  |
| Average beam power per beam              | $P_{\text{ave}}$        | 2.1  | 2.6   | 3.7   | 5.3   | 10.5     | 13.6      | 13.6       | MW  |
| Geometric luminosity                     | $L_{\text{geom}}$       | 0.30   | 0.37  | 0.52  | 0.75  | 1.50     | 1.77      | 2.64       | $\times 10^{34} \text{ cm}^{-2} \text{ s}^{-1}$ |
| – with enhancement factor                |                         | 0.50   | 0.68  | 0.88  | 1.47  | 2.94     | 2.71      | 4.32       | $\times 10^{34} \text{ cm}^{-2} \text{ s}^{-1}$ |
| Beamstrahlung parameter (av.)            | $\Upsilon_{\text{ave}}$ | 0.013  | 0.020 | 0.030 | 0.062 | 0.062    | 0.127     | 0.203      |   |
| Beamstrahlung parameter (max.)           | $\Upsilon_{\text{max}}$ | 0.031  | 0.048 | 0.072 | 0.146 | 0.146    | 0.305     | 0.483      |   |
| Simulated luminosity (incl. waist shift) | $L$                     | 0.56   | 0.75  | 1.0   | 1.8   | 3.6      | 3.6       | 4.9        | $\times 10^{34} \text{ cm}^{-2} \text{ s}^{-1}$ |
| Luminosity fraction within 1 %           | $L_{1\%}/L$             | 91   | 87    | 77    | 58    | 58       | 59        | 45         | %   |
| Energy loss from BS                      | $\delta E_{\text{BS}}$  | 0.65   | 0.97  | 1.9   | 4.5   | 4.5      | 5.6       | 10.5       | %   |
| $e^+e^-$ pairs per bunch crossing        | $n_{\text{pairs}}$      | 45   | 62    | 94    | 139   | 139      | 201       | 383        | $\times 10^3$                                   |
| Pair energy per B.C.                     | $E_{\text{pairs}}$      | 25   | 47    | 115   | 344   | 344      | 1338      | 3441       | TeV   |

# Dump line $L^*$ options

Three  $L^*$  configurations have been previously designed for the dump line. Free space downstream of IP in these cases is  $L_{ex}^* = 5.5$  m, 5.95 m, 6.3 m corresponding to the FF  $L^* = 3.51$  m, 4.0 m, 4.5 m. Only QDEX1 changes position in these dump line options. This study is performed for the dump line option with  $L_{ex}^* = 6.3$  m ( $L^* = 4.5$  m).

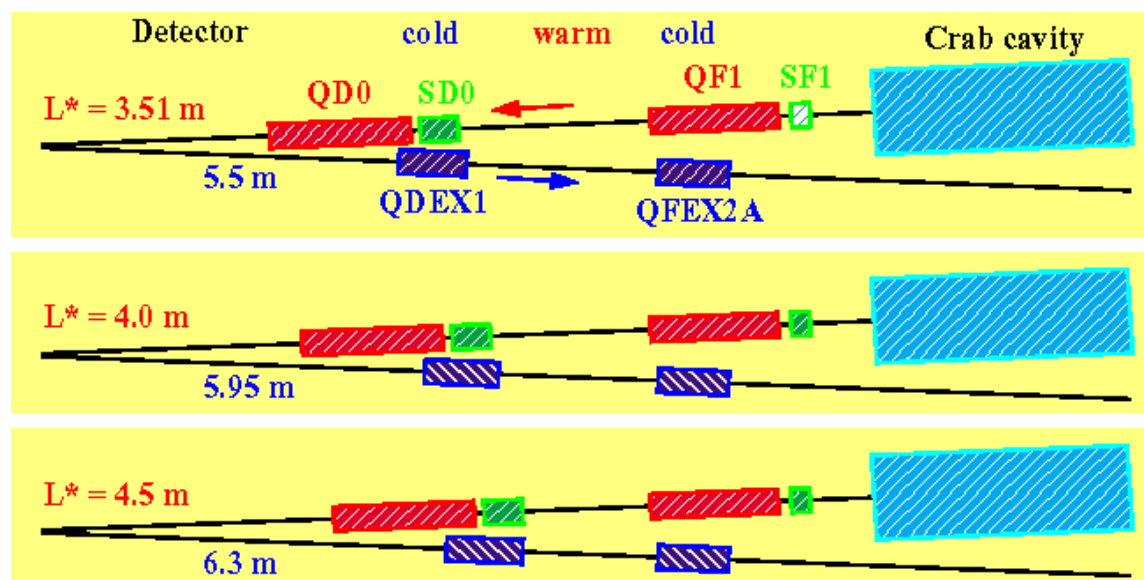
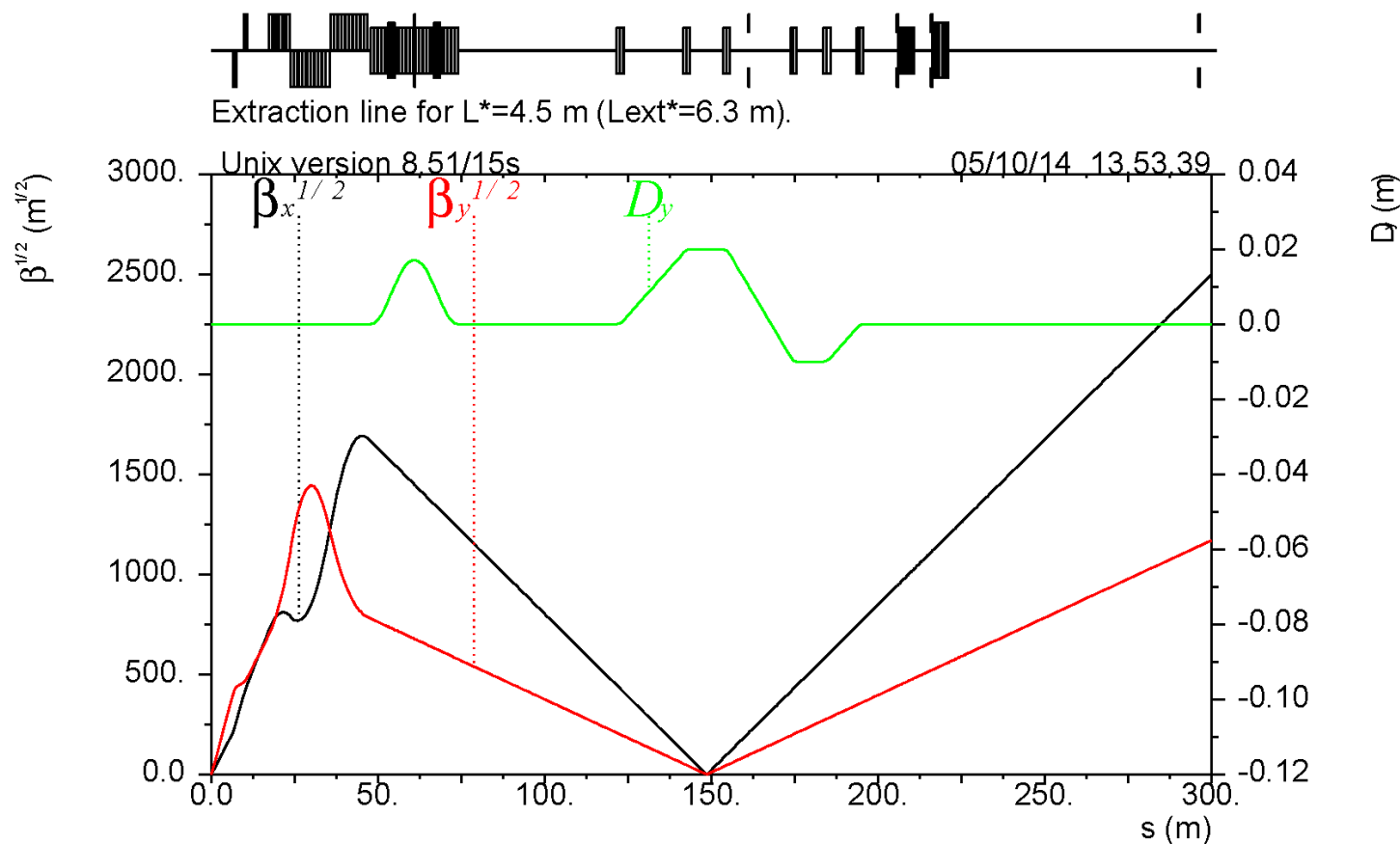


Table 1: Quadrupole gradient (T/m), length (m) and aperture radius (mm) at 500 GeV CM.

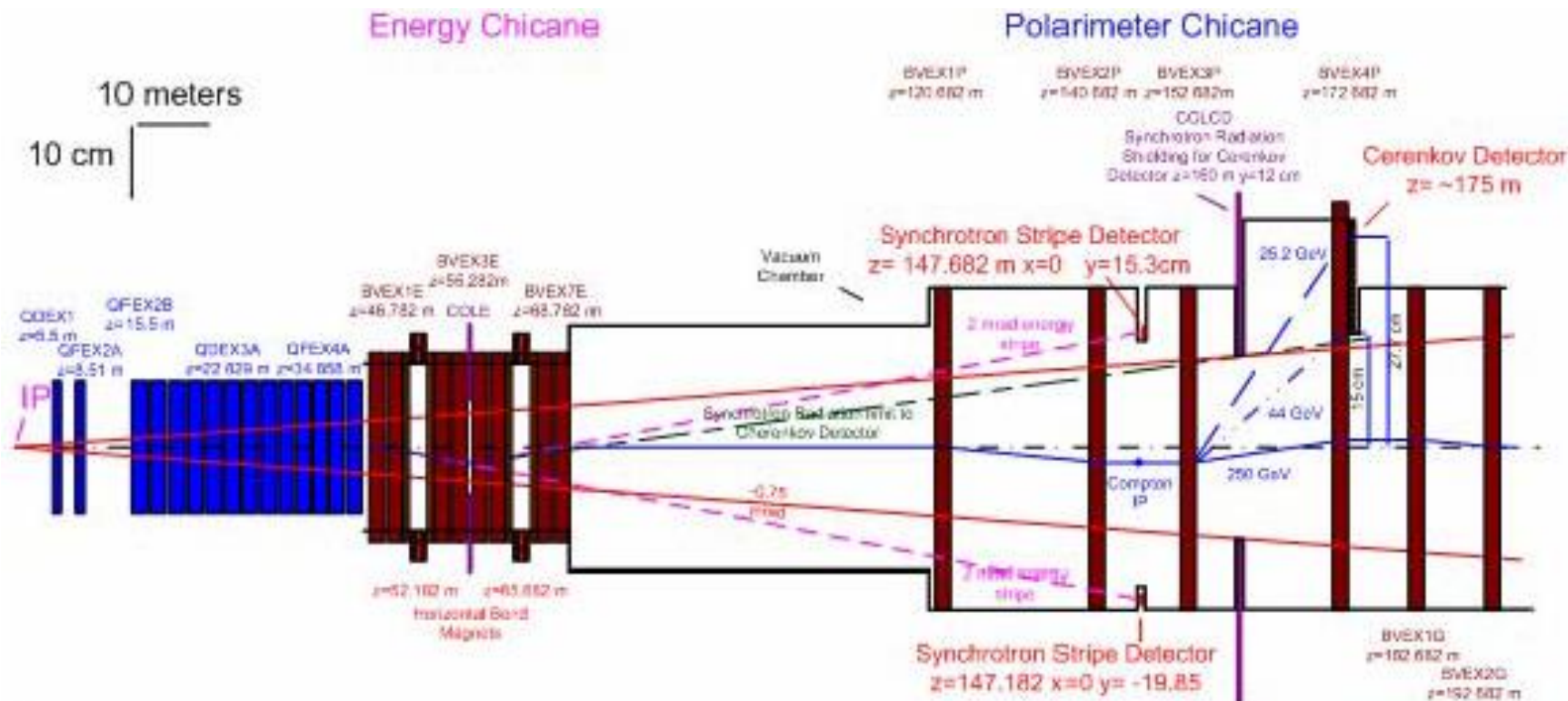
| Name            | Qty | $L^* = 3.51$ m |       |    | $L^* = 4.0$ m |       |    | $L^* = 4.5$ m |       |    |
|-----------------|-----|----------------|-------|----|---------------|-------|----|---------------|-------|----|
|                 |     | B'             | L     | R  | B'            | L     | R  | B'            | L     | R  |
| QDEX1 (SC)      | 1   | 98.00          | 1.060 | 15 | 89.41         | 1.150 | 17 | 86.39         | 1.190 | 18 |
| QFEX2A (SC)     | 1   | 31.33          | 1.100 | 30 | 33.67         | 1.100 | 30 | 36.00         | 1.100 | 30 |
| QFEX2 (B,C,D)   | 3   | 11.12          | 1.904 | 44 | 11.27         | 1.904 | 44 | 11.36         | 1.904 | 44 |
| QDEX3 (A,B,C)   | 3   | 11.39          | 2.083 | 44 | 11.37         | 2.083 | 44 | 11.36         | 2.083 | 44 |
| QDEX3D          | 1   | 9.82           | 2.083 | 51 | 9.81          | 2.083 | 51 | 9.80          | 2.083 | 51 |
| QDEX3E          | 1   | 8.21           | 2.083 | 61 | 8.20          | 2.083 | 61 | 8.19          | 2.083 | 61 |
| QFEX4A          | 1   | 7.05           | 1.955 | 71 | 7.04          | 1.955 | 71 | 7.04          | 1.955 | 71 |
| QFEX4 (B,C,D,E) | 4   | 5.89           | 1.955 | 85 | 5.88          | 1.955 | 85 | 5.88          | 1.955 | 85 |

# Dump line optics with $L_{ex}^* = 6.3$ m

The dump line includes quadrupoles focusing the beam to a second focal point (at ~150 m from IP), two chicanes (for energy, polarimetry and GamCal diagnostics), fast kickers for sweeping beam at dump window, and 5 collimators to protect the diagnostics and remove the beam halo before the dump. The shown  $\beta$ -functions correspond to 500 GeV disrupted beam (solenoid off).



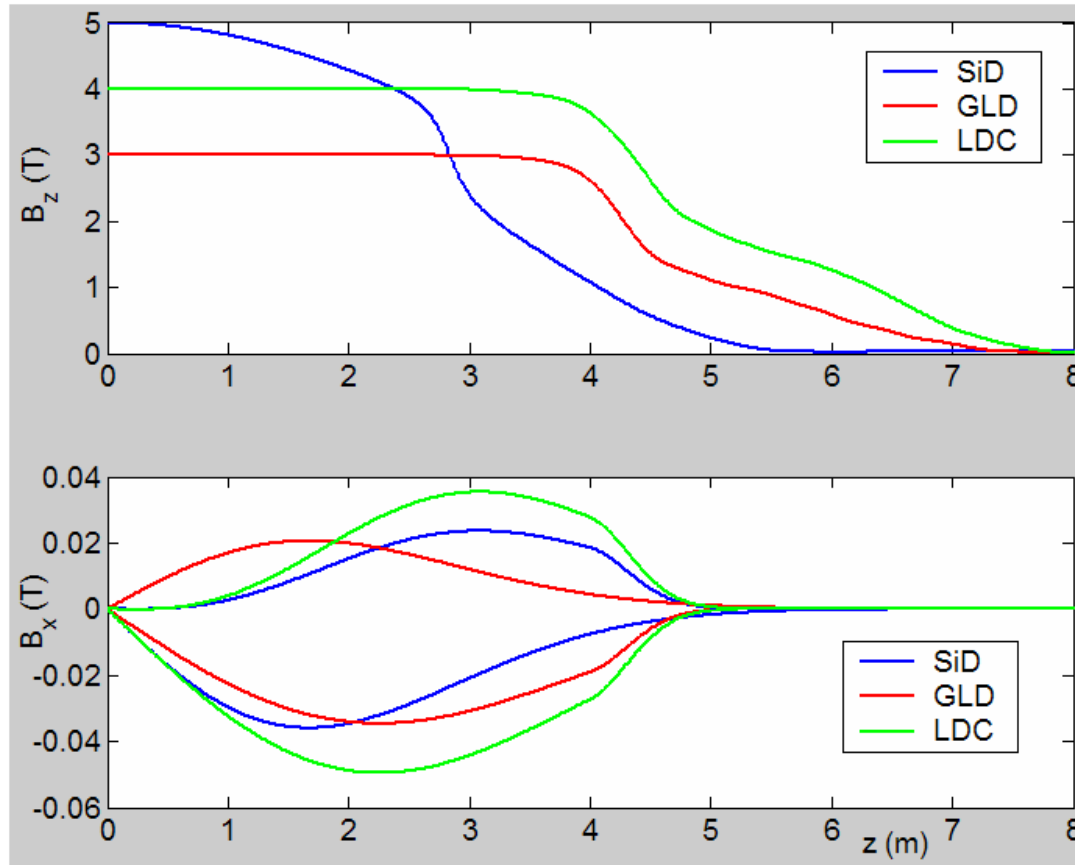
# Chicane diagnostics



This schematic shows locations of the SR detector for energy diagnostics and Cherenkov detector for polarimetry. The Gamma Calorimeter location is after the last chicane bend. The proposed vacuum chamber is accepting IP photon angles up to  $\pm 0.75$  mrad before the final collimation.

K. Moffeit

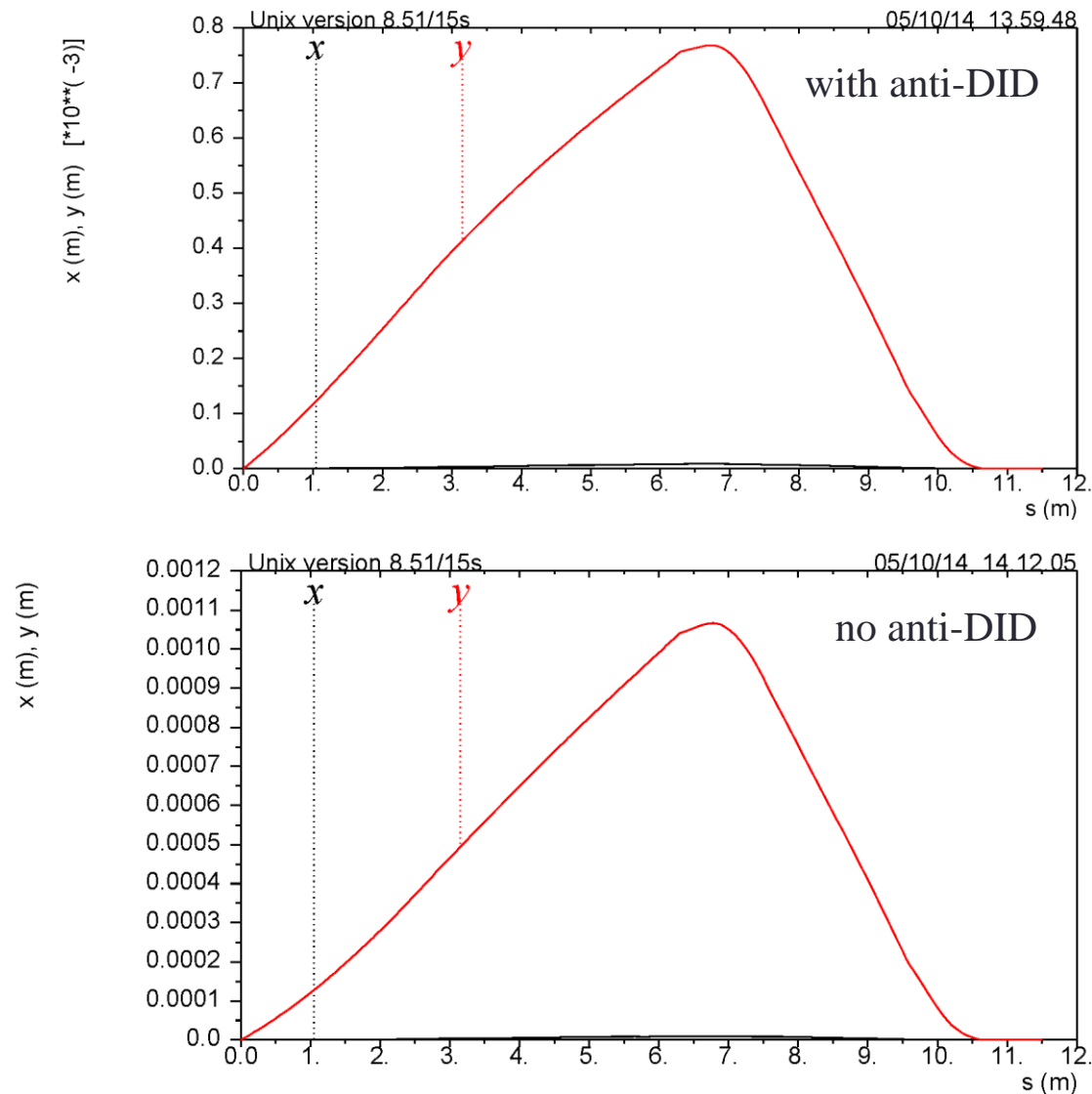
# Solenoid and anti-DID



SiD solenoid field model is used in the simulations with and without anti-DID correcting horizontal field

Figure 8: Top plot: detector fields. Bottom plot: field of anti-DID (positive curves) in comparison with DID (negative curves) for 14mrad crossing angles. The DID field corresponds to earlier results, where flattening of the field in the central region was not yet implemented.

# Solenoid orbit correction with and w/o anti-DID

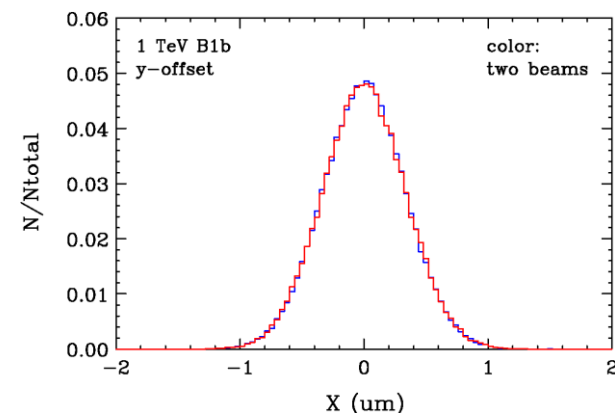
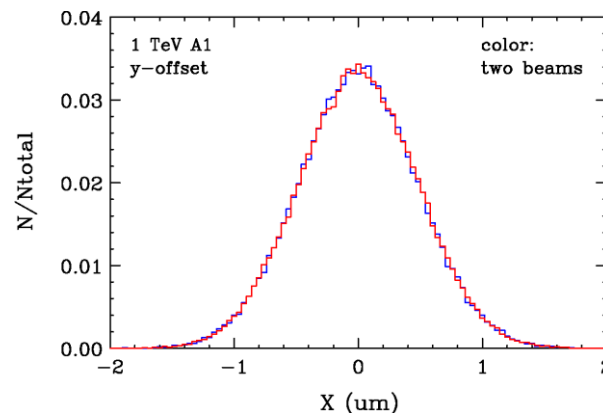
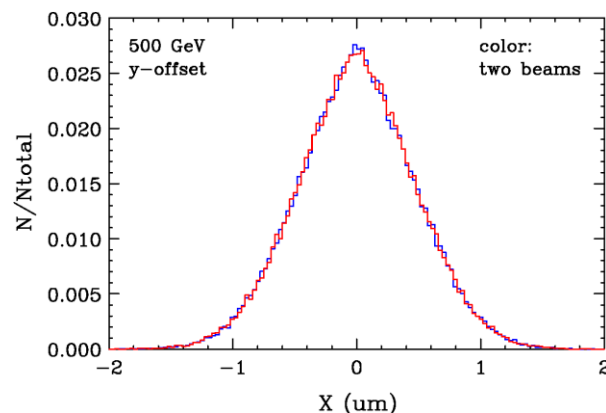
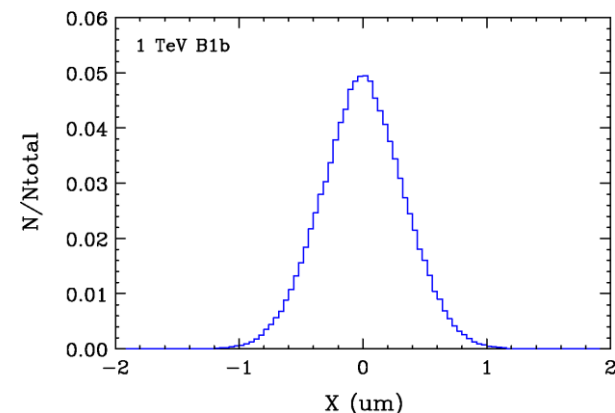
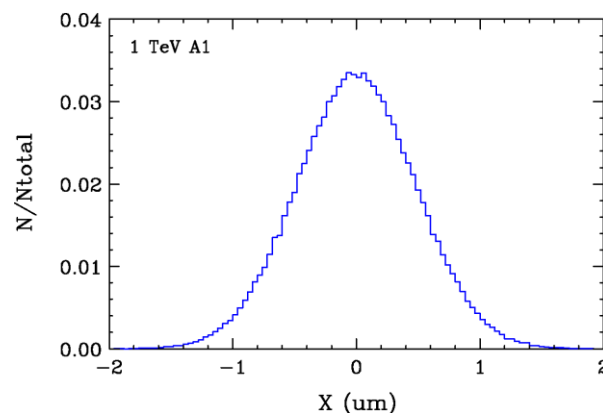
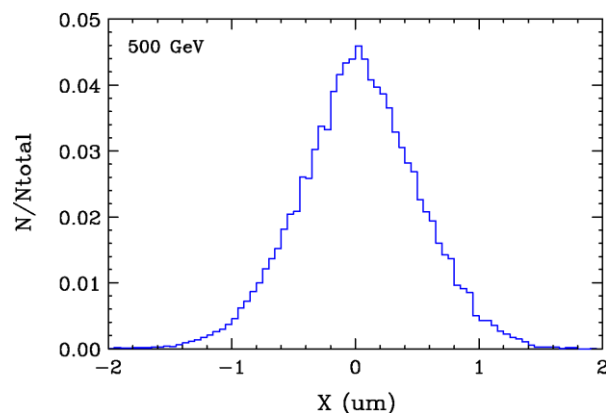


- Solenoid at a horizontal angle with respect to the beam results in a vertical orbit. This orbit is locally cancelled using corrector coils on the first two SC extraction quads.
- The anti-DID field reduces both the solenoid orbit and the background of outgoing secondary particles in the detector.
- The simulations included two options: with and without the anti-DID field.
- Additional conservative assumption used in the simulations is a **non-zero incoming vertical orbit angle at IP** (e.g. due to optimization of upstream orbit and SR effects): **100  $\mu$ rad at 500 GeV and 50  $\mu$ rad at 1 TeV.**



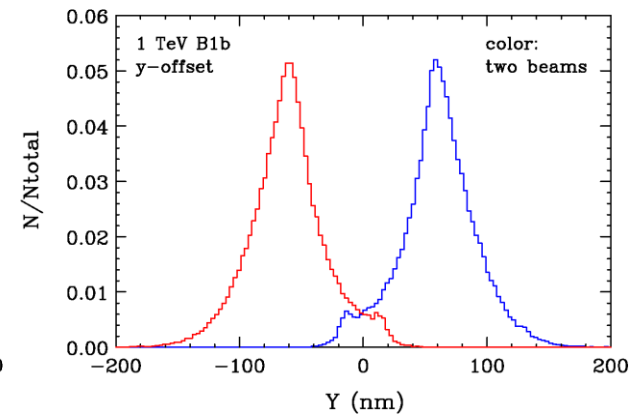
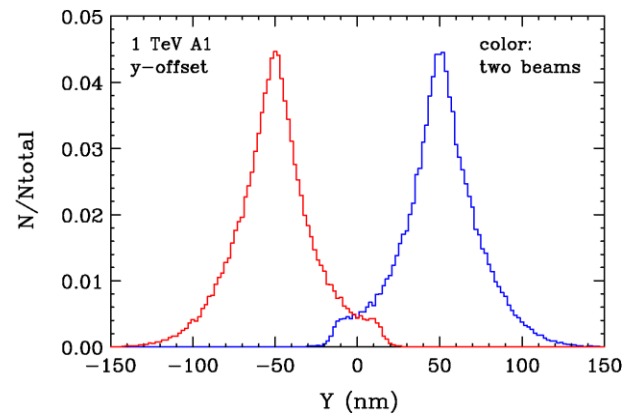
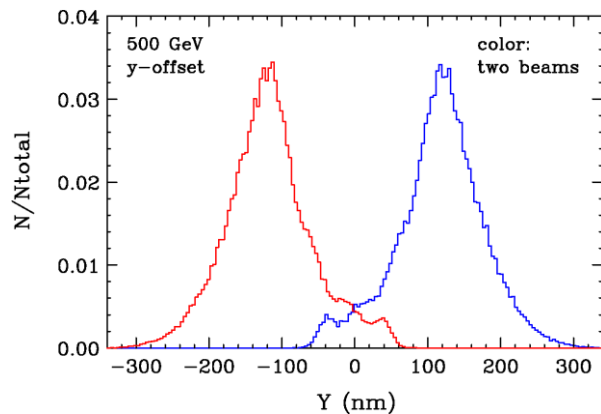
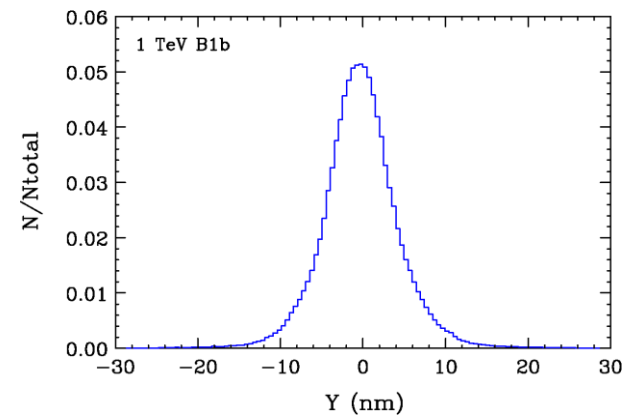
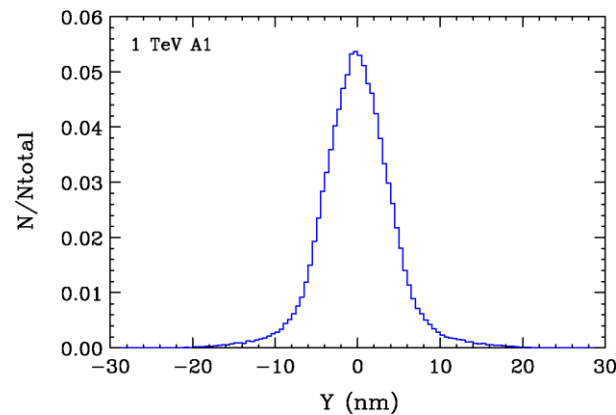
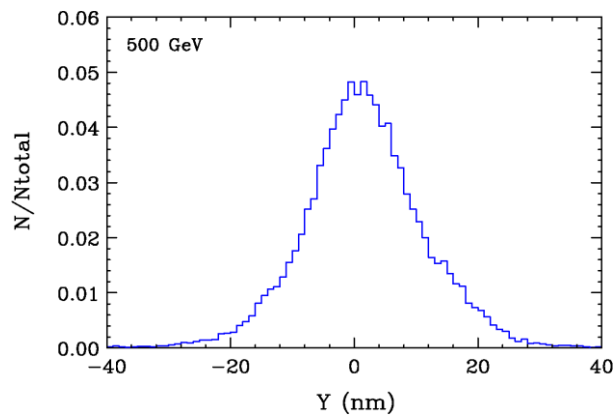
# Disrupted electron horizontal size at IP

- Comparable x-size of the 500 GeV nominal and 1 TeV A1 beams, smaller x-size of 1 TeV B1b beam.
- Comparable sizes with and without IP y-offset.



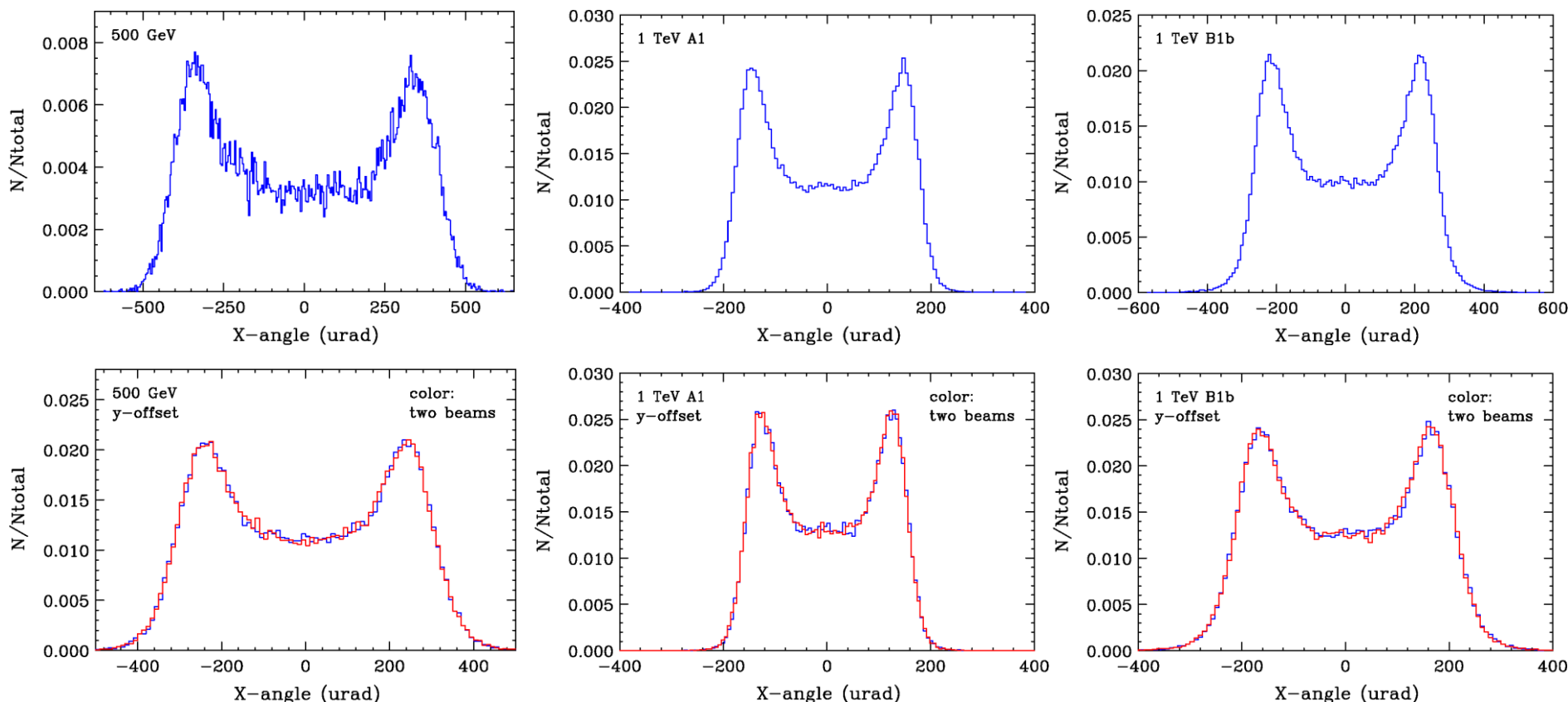
# Disrupted electron vertical size at IP

- Smaller y-size at 1 TeV.
- Systematic offset between two beams and larger y-spread with IP y-offset.
- Much smaller y-size versus x-size.



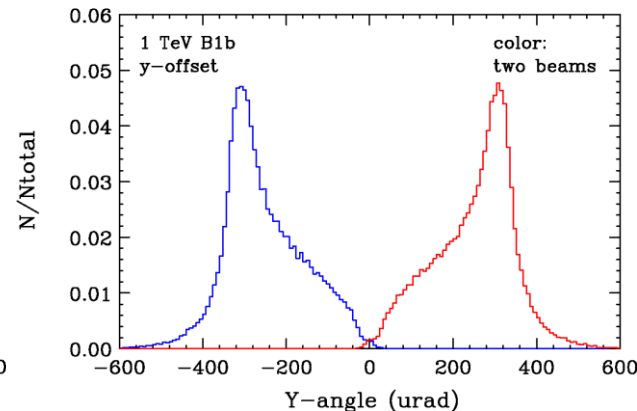
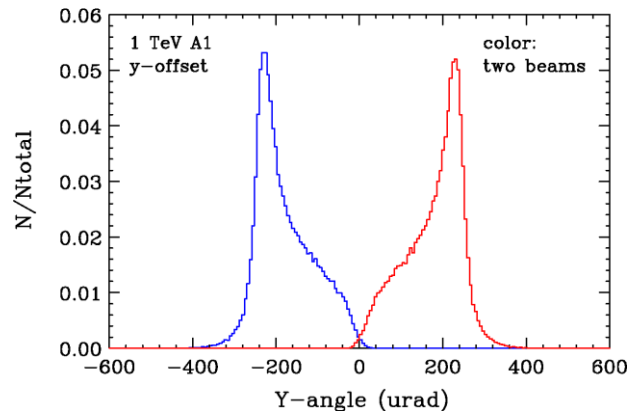
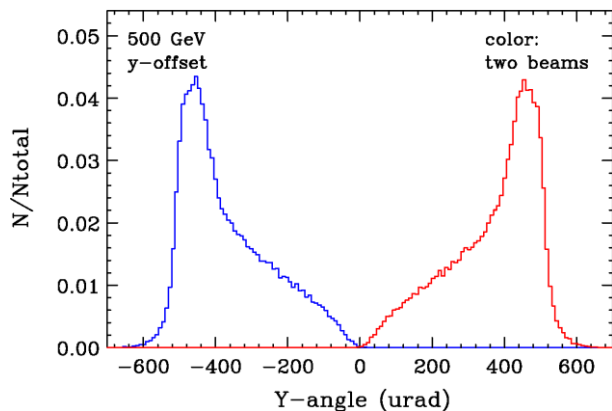
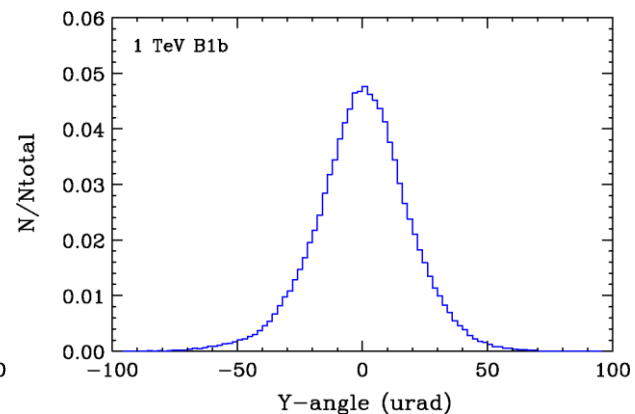
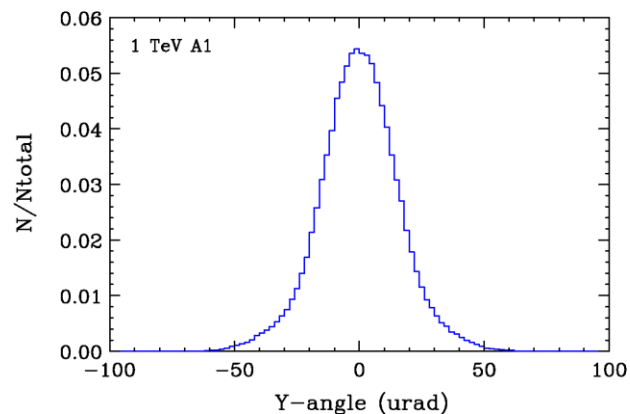
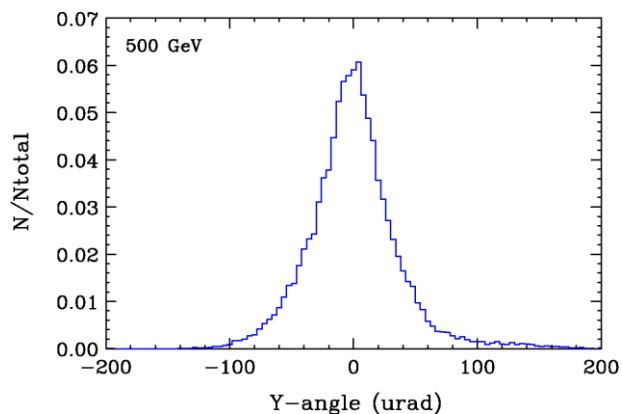
# Disrupted electron horizontal angular spread at IP

- Largest x-angles at 500 GeV.
- Somewhat smaller x-angles with the IP y-offset.
- Angles larger than 0.5 mrad may lead to losses in the dump line.



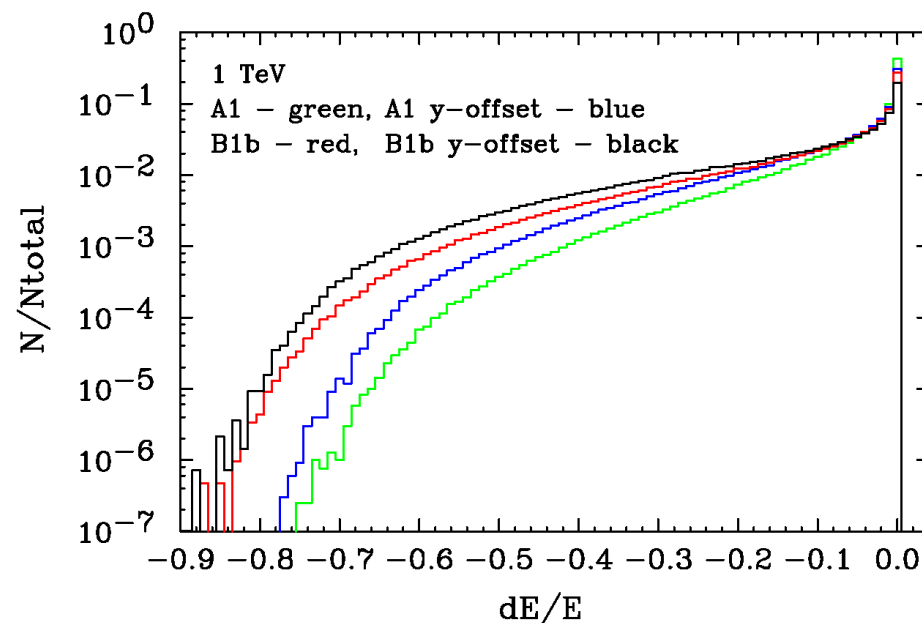
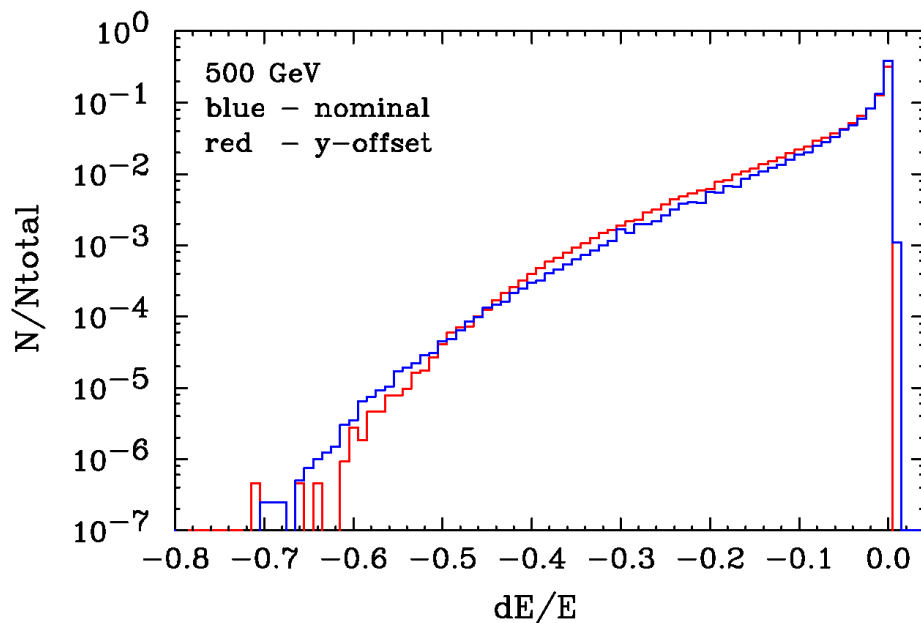
# Disrupted electron vertical angular spread at IP

- Larger y-angles at 500 GeV versus 1 TeV.
- Systematic ( $\pm$ ) offset and larger y-angles with the IP y-offset.
- Much smaller y-angles versus x-angles at nominal collisions, but comparable with IP y-offset.
- With the IP y-offset the losses of the two beams will be unequal since the vertical chicane dispersion will add up with the orbits of one sign of the IP angle, but not with the other.



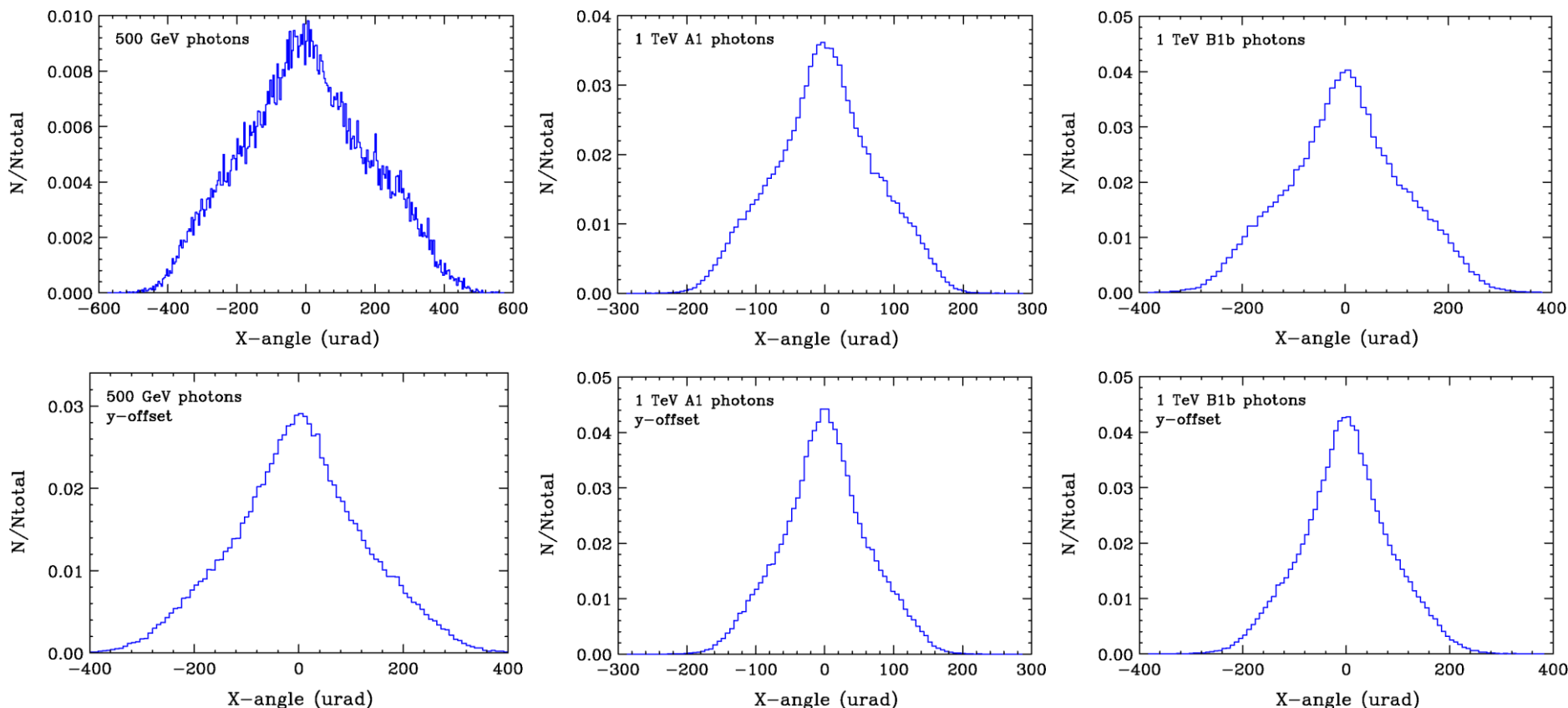
# Disrupted electron energy spread at IP

- 500 GeV: comparable distributions with and without IP y-offset.
- 1 TeV: a longer low energy tail in B1b option (i.e. expect higher beam loss), the energy tail is further increased with the IP y-offset.



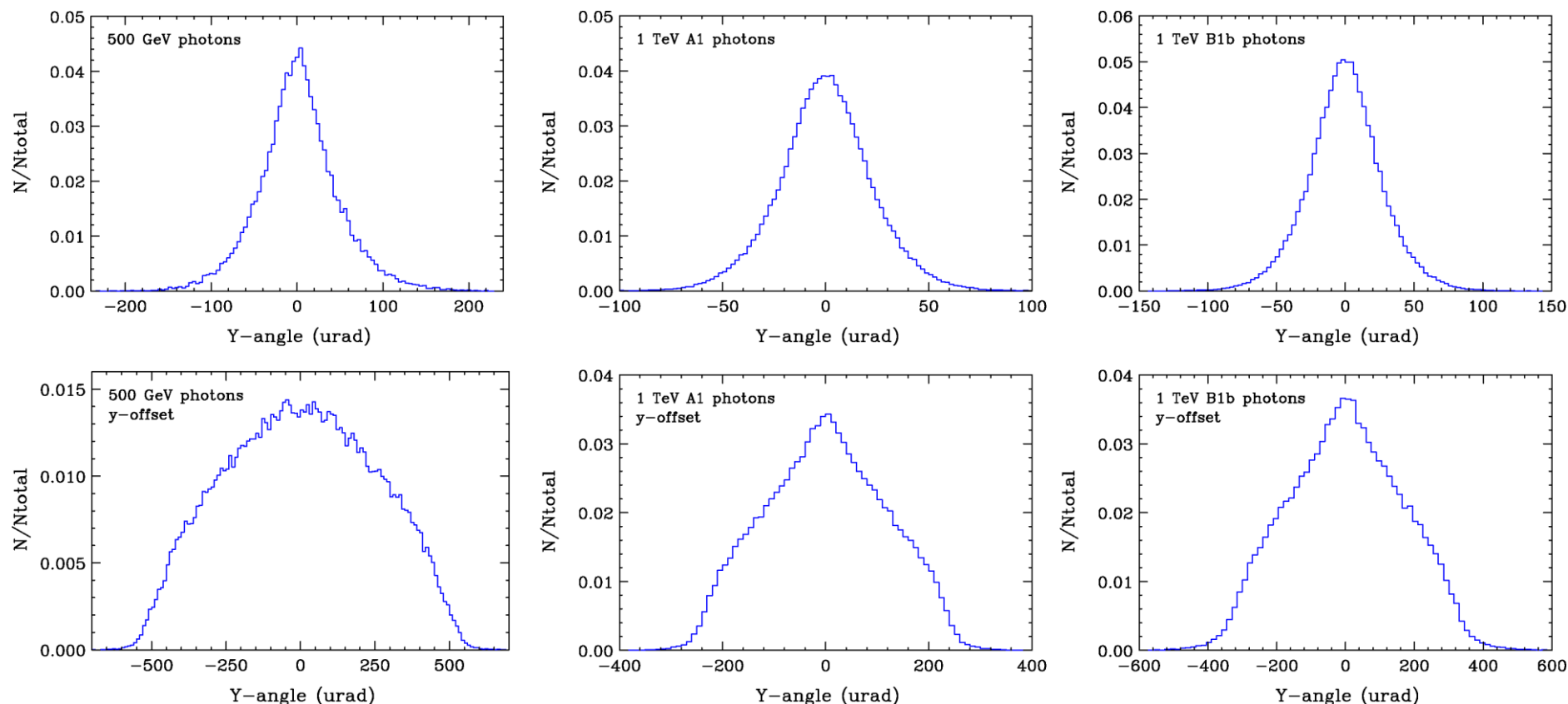
# Beamstrahlung photon horizontal angular spread at IP

- Larger x-angles at 500 GeV versus 1 TeV.
- Somewhat smaller x-angles with the IP y-offset.
- The dump line collimator acceptance is  $\pm 0.5$  mrad.



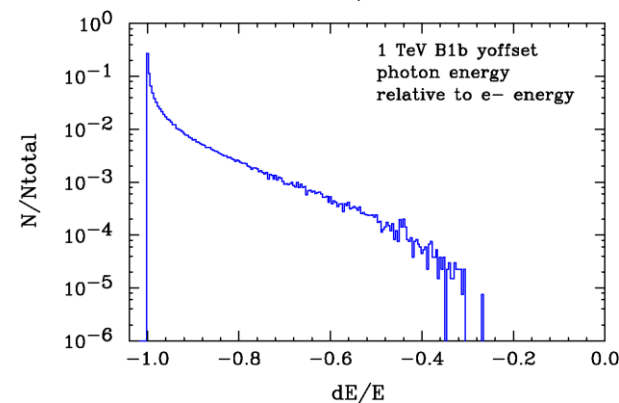
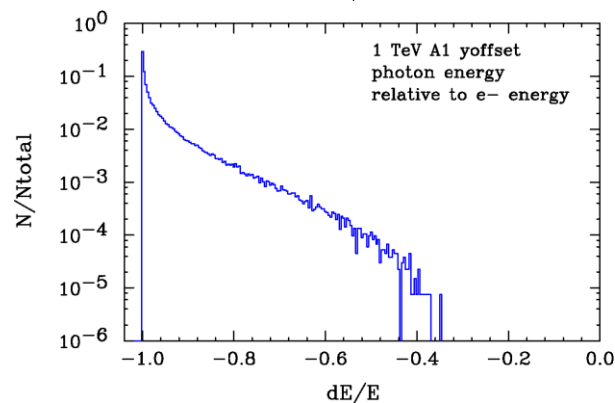
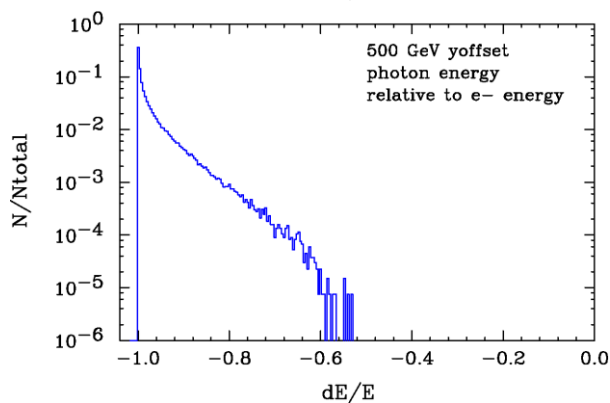
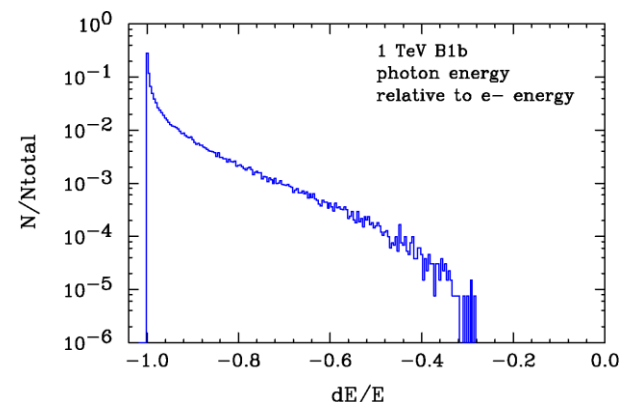
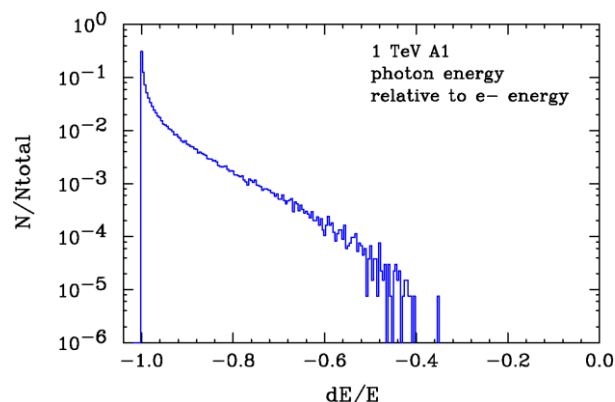
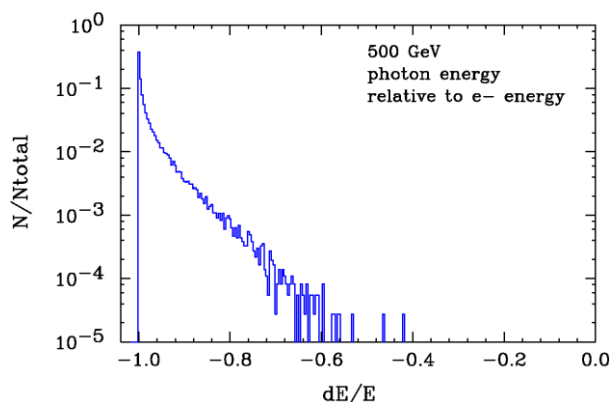
# Beamstrahlung photon vertical angular spread at IP

- Larger y-angles at 500 GeV versus 1 TeV.
- Much larger y-angles with the IP y-offset.
- Much smaller y-angles versus x-angles at nominal collisions, but somewhat larger with the y-offset.



# Beamstrahlung photon energy spread

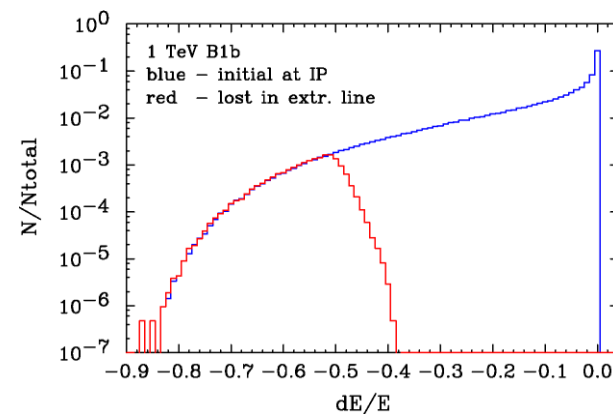
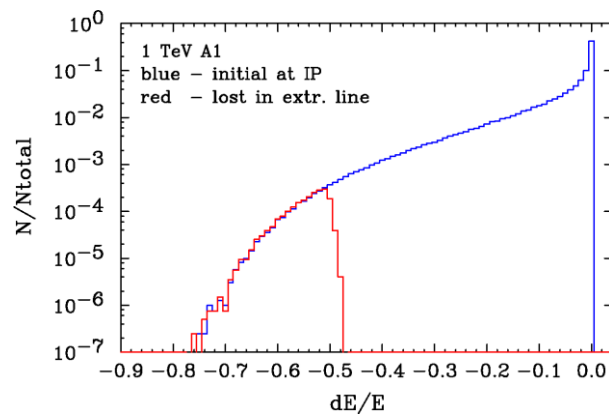
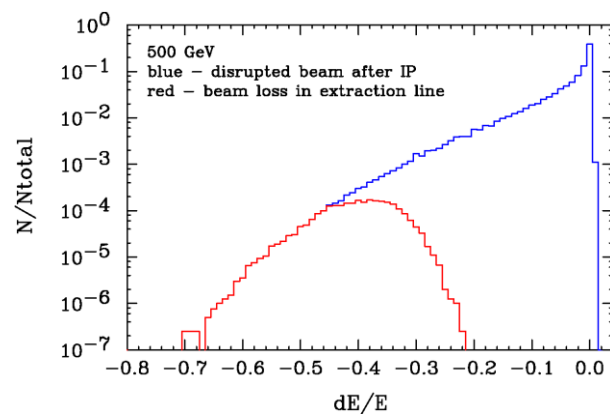
- Longer high energy tail at 1 TeV versus 500 GeV.
- Longer high energy tail in B1b option versus A1 at 1 TeV.
- Comparable energy tails with and without IP y-offset.





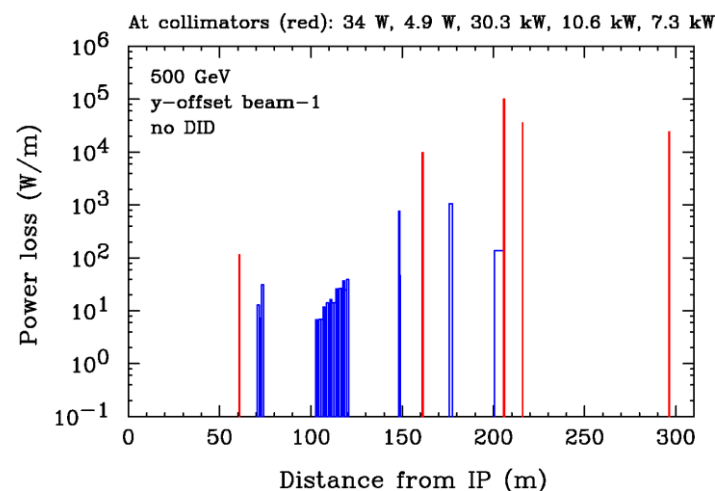
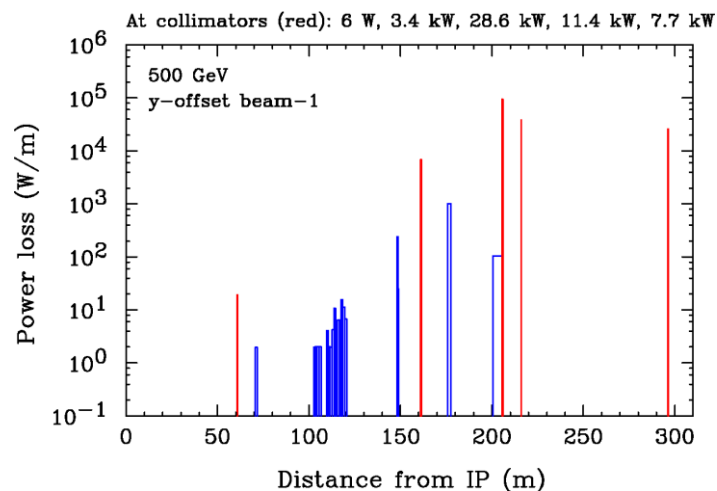
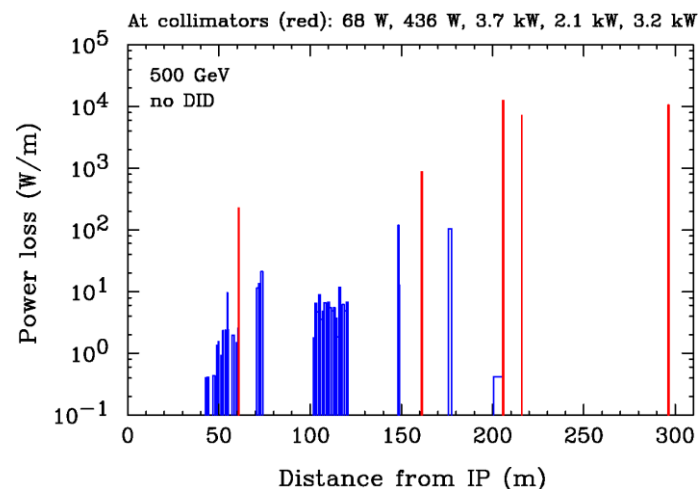
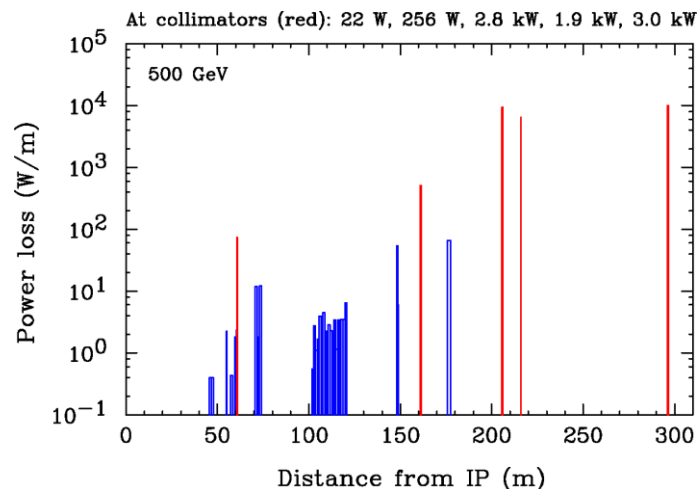
# Energy of electrons lost in the dump line (head-on)

- Most electrons are lost due to low energy ( $<70\%$  of the nominal energy).
- A smaller fraction is lost due to large IP angles ( $>0.5$  mrad) as at 500 GeV in the figure below.



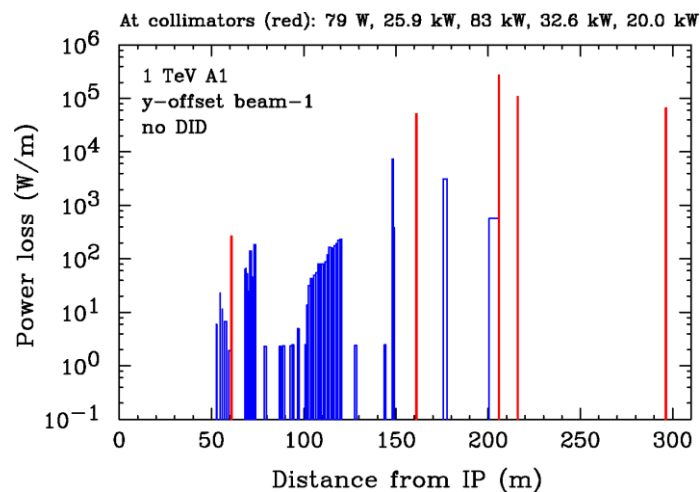
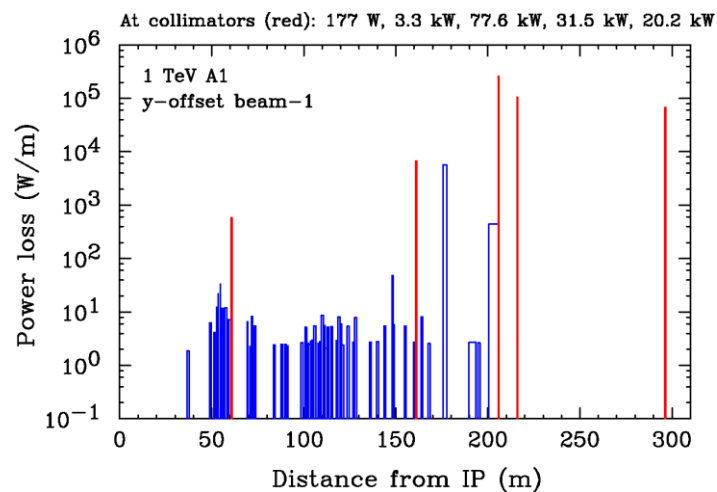
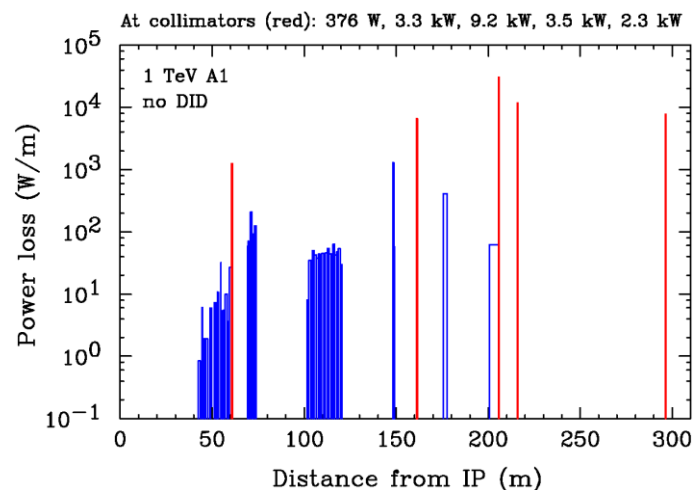
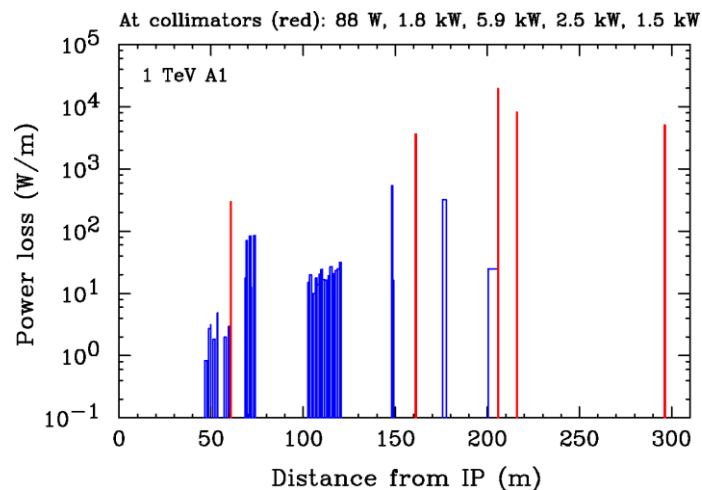
# Electron power loss at 500 GeV CM

- Head-on: the losses  $< 100$  W/m in magnets and pipe – should be acceptable (N. Mokhov).
- Somewhat higher losses without anti-DID than with anti-DID.
- Much higher losses in collimators for one of the beams with the IP y-offset.



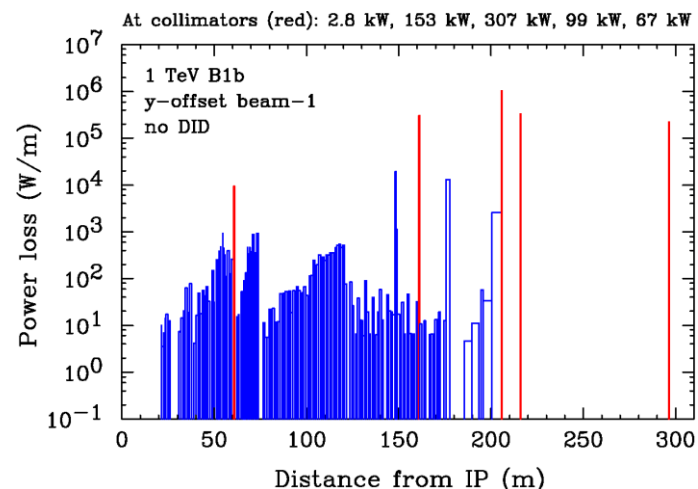
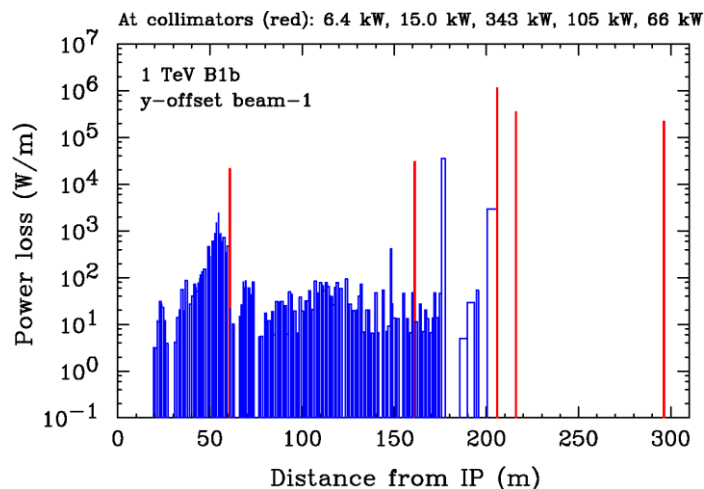
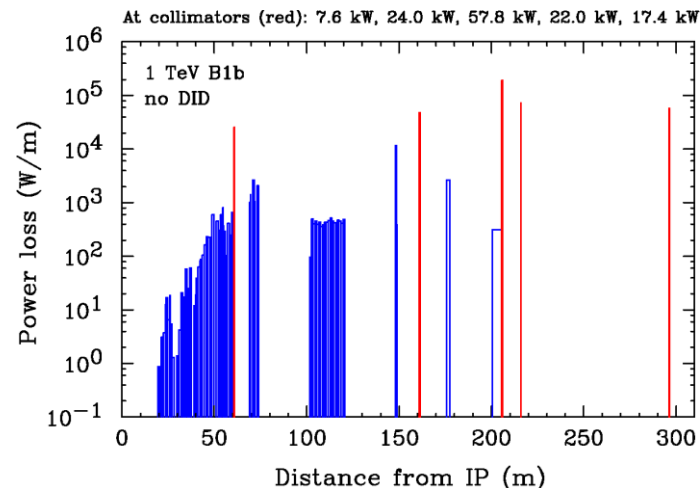
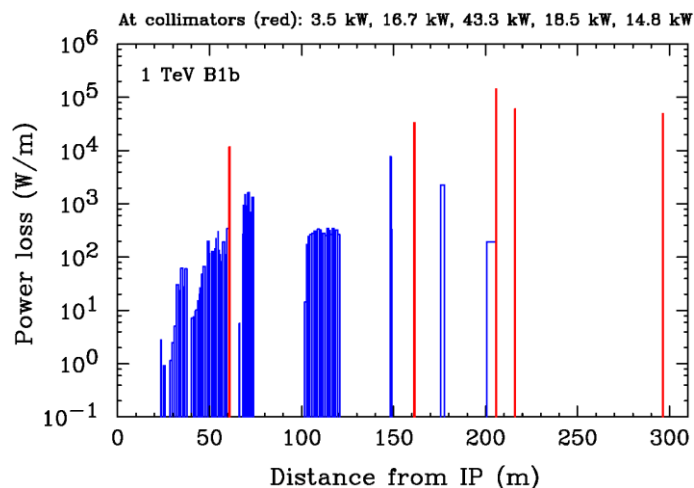
# Electron power loss in option A1 at 1 TeV CM

- Head-on losses: mostly  $< 100$  W/m in magnets/pipe – may be acceptable.
- Somewhat higher losses without anti-DID.
- Much higher losses in collimators for one of the beams with the IP y-offset.



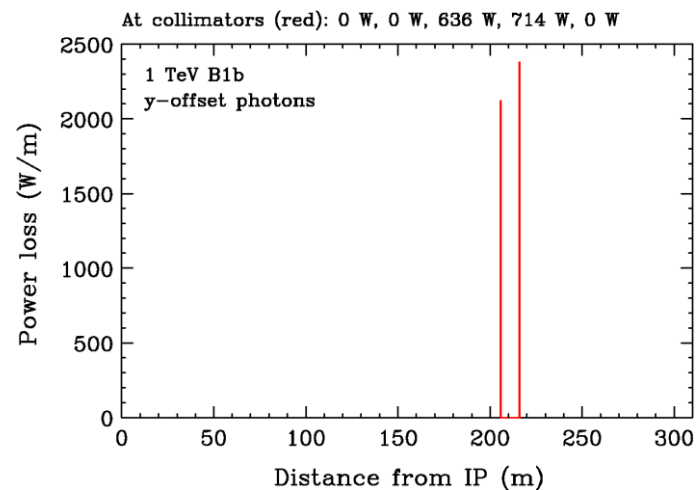
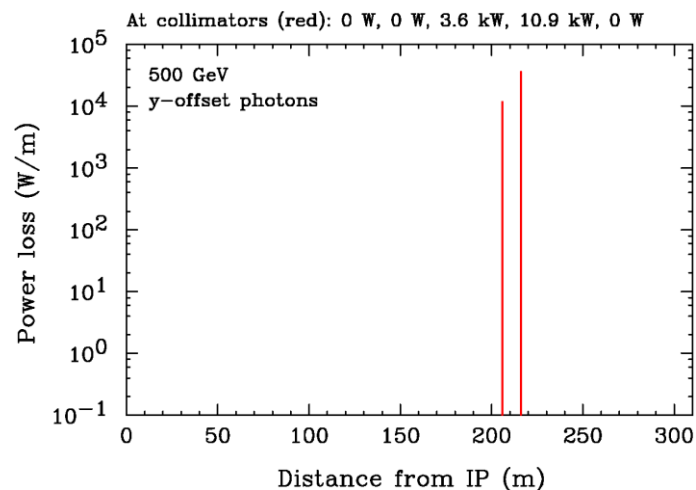
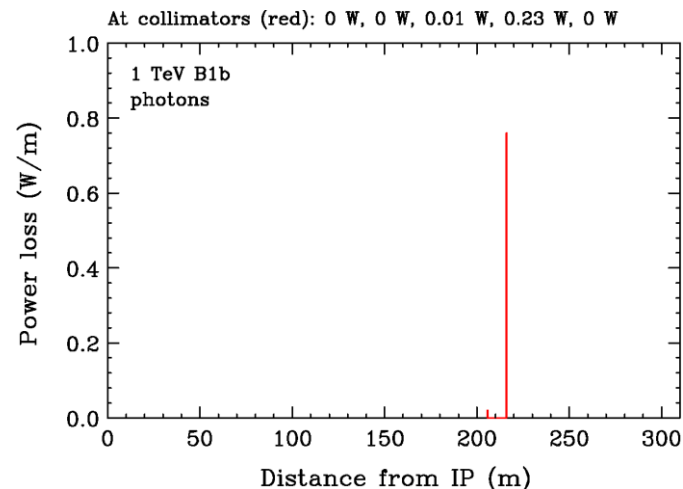
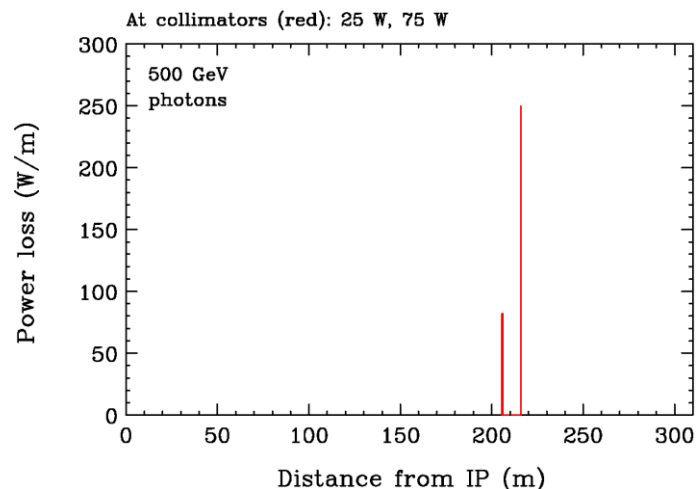
# Electron power loss in option B1b at 1 TeV CM

- Head-on losses:  $\sim 1$  kW/m in magnets/pipe and  $\sim 40$  kW in collimators – appear unacceptable.
- Somewhat higher losses without anti-DID.
- Much higher losses in collimators for one of the beams with IP y-offset.



# Beamstrahlung photon loss

- Head on: very small losses, limited to collimators.
- No photon loss in option A1 at 1 TeV (with and without y-offset)
- Higher losses with the IP y-offset, limited to 2 collimators – should be acceptable.



## Summary of electron beam loss (head-on)

| Parameter option  | Warm magnets | Pipe     | Detectors   |           | Collimators |           |         |         |         |
|-------------------|--------------|----------|-------------|-----------|-------------|-----------|---------|---------|---------|
|                   |              |          | Synchrotron | Cherenkov | Energy      | Cherenkov | Dump-1  | Dump-2  | Dump-3  |
| 500 GeV           | 12 W/m       | 5 W/m    | 30 W        | 132 W     | 22 W        | 256 W     | 2.8 kW  | 1.9 kW  | 3.0 kW  |
| 500 GeV w/o DID   | 21 W/m       | 14 W/m   | 66 W        | 209 W     | 68 W        | 436 W     | 3.7 kW  | 2.1 kW  | 3.2 kW  |
| 1 TeV A1          | 85 W/m       | 48 W/m   | 279 W       | 642 W     | 88 W        | 1.8 kW    | 5.9 kW  | 2.5 kW  | 1.5 kW  |
| 1 TeV A1 w/o DID  | 206 W/m      | 92 W/m   | 679 W       | 819 W     | 376 W       | 3.3 kW    | 9.2 kW  | 3.5 kW  | 2.3 kW  |
| 1 TeV B1b         | 1.6 kW/m     | 0.9 kW/m | 4.0 kW      | 4.6 kW    | 3.5 kW      | 16.7 kW   | 43.3 kW | 18.5 kW | 14.8 kW |
| 1 TeV B1b w/o DID | 2.7 kW/m     | 1.4 kW/m | 5.9 kW      | 5.3 kW    | 7.6 kW      | 24.0 kW   | 57.8 kW | 22.0 kW | 17.4 kW |

- Per N. Mokhov: for electron beam ~100 W/m in pipe and ~1 kW/m in warm magnets should be acceptable in terms of radiation dose.
- Highlighted values considered unacceptable.
- No loss in SC quads.
- Losses in diagnostic detectors need to be evaluated by a diagnostic expert.

# Conclusions

- Electron beam loss in head-on collisions at 500 GeV and in option A1 at 1 TeV are considered acceptable, but an expert opinion is needed to evaluate losses in diagnostic detectors. A tighter collimation may be needed.
- Beam loss in option B1b is high due to the long beam energy tail and is likely unacceptable.
- Beam loss without anti-DID field is somewhat increased (up to a factor of 2).
- The high losses with the IP y-offset are expected to be only for short periods of time, therefore should be manageable. The IP offsets will be continuously corrected in operation.
- Power losses of beamstrahlung photons are small (acceptable) and limited to two dump collimators.